HOLOGIC®
The Science of Sure

Powerful images.
Clear answers.

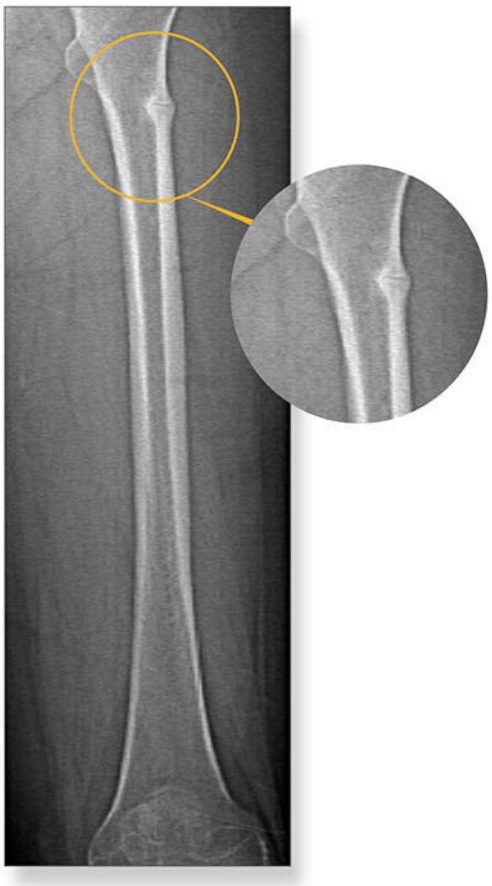

Manage Patient's concerns about Atypical Femur Fracture*

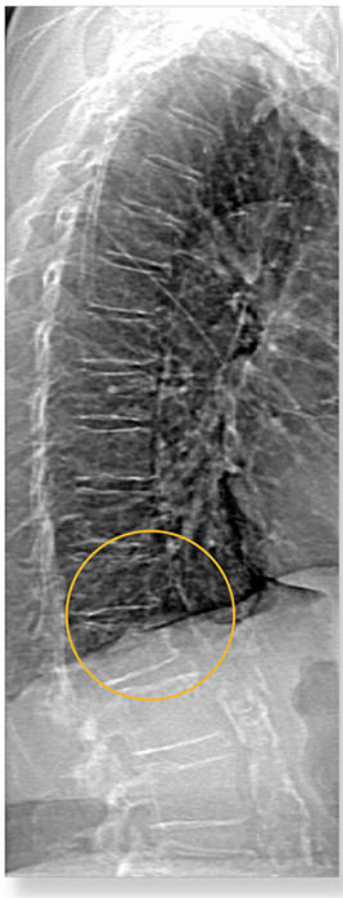

Vertebral Fracture Assessment – a critical part of a complete fracture risk assessment

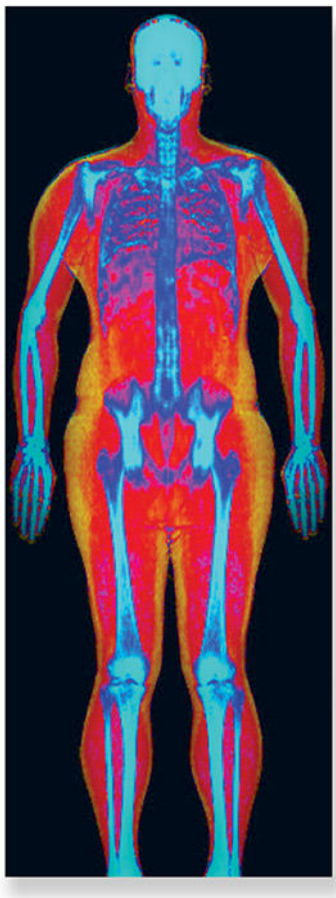

Advanced Body Composition® Assessment – the power to see what's inside

Contact your Hologic rep today at insidesales@hologic.com

*Incomplete Atypical Femur Fractures imaged with a Hologic densitometer, courtesy of Prof. Cheung, University of Toronto

www.hologic.com | info@hologic.com | 1.781.999.7300

ORIGINAL ARTICLE

JBMR®

Attenuation of NF-κB in Intestinal Epithelial Cells Is Sufficient to Mitigate the Bone Loss Comorbidity of Experimental Mouse Colitis

Ke Ke,[1] Tim (Hung-Po) Chen,[1] Manoj Arra,[1] Gabriel Mbalaviele,[2] Gaurav Swarnkar,[1] and Yousef Abu-Amer[1,3]*

[1]Department of Orthopaedic Surgery and Cell Biology and Physiology, Washington University School of Medicine, St. Louis, MO, USA
[2]Bone and Mineral Division, Department of Medicine, Washington University School of Medicine, St. Louis MO, USA
[3]Shriners Hospital for Children, St. Louis, MO, USA

ABSTRACT

Skeletal abnormalities are common comorbidities of inflammatory bowel disease (IBD). Patients suffering from IBD, including ulcerative colitis and Crohn's disease, present with skeletal complications. However, the mechanism underpinning IBD-associated bone loss remains vague. Intestinal inflammation generates an inflammatory milieu at the intestinal epithelium that leads to dysregulation of mucosal immunity through gut-residing innate lymphoid cells (ILCs) and other cell types. ILCs are recently identified mucosal cells considered as the gatekeeper of gut immunity and their function is regulated by intestinal epithelial cell (IEC)-secreted cytokines in response to the inflammatory microenvironment. We first demonstrate that serum as well as IECs collected from the intestine of dextran sulfate sodium (DSS)-induced colitis mice contain high levels of inflammatory and osteoclastogenic cytokines. Mechanistically, heightened inflammatory response of IECs was associated with significant intrinsic activation of NF-κB (nuclear factor kappa-light-chain-enhancer of activated B cells) in IECs and increased frequency of ILC1, ILC3, and myeloid osteoclast progenitors. Validating the central role of IEC-specific NF-κB activation in this phenomenon, conditional expression of constitutively active inhibitor kappa B kinase 2 (IKK2) in IECs in mice recapitulates the majority of the cellular, inflammatory, and osteolytic phenotypes observed in the chemically induced colitis. Furthermore, conditional deletion of IKK2 from IECs significantly attenuated inflammation and bone loss in DSS-induced colitis. Finally, using the DSS-induced colitis model, pharmacologic inhibition of IKK2 was effective in reducing frequency of ILC1 and ILC3 cells, attenuated circulating levels of inflammatory cytokines, and halted colitis-associated bone loss. Our findings identify IKK2 in IECs as viable therapeutic target for colitis-associated osteopenia. © 2019 American Society for Bone and Mineral Research.

KEY WORDS: BONE LOSS; INFLAMMATION; NF-κB; INTESTINE; ILCS; IECS; COLITIS

Introduction

Bone homeostasis is tightly regulated by osteoclasts and osteoblasts.[1] Numerous immune cells and factors contribute to homeostasis of this process, while imbalanced activity of these cells in pathologic states uncouples bone resorption and bone formation, leading to skeletal anomalies. It has been long established that inflammatory insults alter bone homeostasis, leading to various skeletal anomalies.[2–7] Although this process is complex, it is apparent that the inflammatory response dysregulates osteoclast and osteoblast differentiation and function, a process that is mediated by pro-inflammatory factors and anti-anabolic modulators. Specifically, inflammatory mediators promote differentiation of myeloid cells into osteoclasts to exacerbate bone resorption and negatively impact bone formation by targeting mesenchymal and osteoblast cells.

At the cellular level, hematopoietic stem cells (HSCs), innate lymphoid cells (ILCs), and other immune cells are activated, leading to elevated levels of pro-inflammatory cytokines including interleukin-23 (IL-23), interleukin-17 (IL-17), granulocyte-macrophage colony-stimulating factor (GM-CSF), granulocyte colony-stimulating factor (G-CSF), tumor necrosis factor α (TNFα), interleukin-1β (IL-1β), and more. This pro-inflammatory milieu mobilizes bone marrow cells to the bloodstream and periphery, thus altering the bone marrow microenvironment and adversely affecting bone cells. In fact, it has been shown that elevated levels of the pro-inflammatory factors TNFα, interferon γ (IFNγ), and G-CSF potently inhibit osteogenesis.[8] In this regard, numerous clinical case reports linked high circulating levels of inflammatory cytokines, including TNFα, IL-1β, IL-17, interleukin-4 (IL-4), interleukin-6 (IL-6) and others, with the bone phenotype of the affected subjects.[9–11] In other

Received in original form January 5, 2019; revised form April 26, 2019; accepted May 9, 2019. Accepted manuscript online Month 00, 2019.
Address correspondence to: Yousef Abu-Amer, PhD, Department of Orthopedic Surgery, Washington University School of Medicine, 660 South Euclid Avenue, Campus Box 8233, St. Louis, MO 63110, USA. E-mail: abuamery@wustl.edu
Additional Supporting Information may be found in the online version of this article.
Journal of Bone and Mineral Research, Month 2019, pp 1–14
DOI: 10.1002/jbmr.3759

studies, elevated levels of sclerostin and Dickkopf WNT signaling pathway inhibitor 1(DKK1), factors driven by inflammation, were reported in animal models of rheumatoid arthritis[12] and in synovial tissue from rheumatoid arthritis patients compared with controls, and bone repair was often delayed or repressed in patients with systemic inflammatory background.[13–15]

A prime example of chronic inflammatory disease with detrimental skeletal consequences is inflammatory bowel disease (IBD).[7,16] In fact, osteoporosis has been considered as a comorbidity in patients suffering from chronic inflammatory diseases, such as rheumatoid arthritis and IBD,[4,6,7,17–20] who typically present with increased fracture risk. The pathogenesis of IBD, which includes Crohn's disease and ulcerative colitis,[2,21,22] remains unclear; however, it is believed to be a consequence of dysregulation of the mucosal immune system, leading to excessive immunologic responses and due to changes in the composition of gut flora. In severe cases, these responses are associated with damaged intestine epithelial barrier. The intestinal epithelium, formed by a monolayer of intestinal epithelial cells (IECs), is a crucial protective physical barrier to maintain intestinal homeostasis. Dysfunction of intestinal epithelium or epithelial cells is associated with dysregulation of the mucosal immune system during the clinical course of IBD patients and experimental IBD models, such as in DSS-treated mice.[23] Immune cells such as macrophages, dendritic cells (DC), type 1 T-helper (Th1) and type 2 T-helper (Th2) lymphocytic cells as well as non-immune cells such as epithelial cells are directly involved in IBD pathogenesis.[2,21,24] A breakthrough in recent years has implicated the inflammatory T-helper cell 17 (Th17) subtype and ILCs as major culprits of IBD pathogenesis. ILCs, as well as ILC-produced cytokines, play a central role during intersection of innate and adaptive immune systems, by coordinating inflammation, immunity, wound healing, and tissue homeostasis, with a wide range of influence from immunology to metabolism to tumor defense.[25,26] In this regard, a genomewide association study (GWAS) identified linkage between ILCs and IBD through the IL-23/IFNγ/IL17/G-CSF axis.[8,27–31] Congruently, we have noted exuberant levels of IL-17A, IFNγ, IL-23, G-CSF, GM-CSF, and numerous other cytokines in the serum of mice with experimental ulcerative colitis. Some of these cytokines have been shown to be produced within Paneth cells of intestinal mucosa and expressed within intestinal epithelial cells (IECs)[32–34] and stimulate cells of the innate immune system (neutrophils, macrophages, and DCs).[8,31]

Interestingly, stimulation of the various cell types during inflammatory states leads in all cases to activation of NF-κB signaling cascade and subsequent production of pro-inflammatory[35–38] and, as we propose, osteoclastic cytokines. At the center of this pathway, the kinase complex containing IKK1, IKK2, and IKKγ/NEMO is crucial for its activity.[39,40] IKK2 activates the classical NF-κB pathway and mediates the vast majority of inflammatory responses.[41–45] Constitutively active IKK2 (IKK2ca) (S177/181E) sustains heightened NF-κB activity and intrinsically recapitulates the inflammatory response.[46–48] In this regard, we have shown that knock-in of this IKK2ca form in the myeloid or mesenchymal lineages in mice induced systemic osteopenia owing to elevated endogenous osteoclastogenesis[46] and inhibition of bone formation,[49] respectively. In the current study, we hypothesized that gut inflammation contributes to systemic bone loss through NF-κB activation in gut-residing immune cells. Indeed, we demonstrate that expression of active IKK2 in gut IECs triggers colitis-like pathology and significant bone loss similar to that associated with the experimental dextran sodium sulfate (DSS)-induced colitis. We further provide direct evidence that genetic ablation of IKK2 in IECs or systemic pharmacologic inhibition of this kinase attenuates experimental colitis-induced bone loss. This finding buttresses the pathogenic role of NF-κB as the principal player that links inflammation (acute and chronic) with systemic bone loss and presents it as a viable therapeutic target.

Materials and Methods

Study design: animals and treatments

The objective of this study was to determine the mechanism underpinning colitis-associated bone loss. Based on our preliminary observations, we tested the hypothesis that IEC-specific activation of NF-κB and subsequently secreted cytokine mediate bone loss associated with murine colitis. We validated this by using multiple in vivo approaches employing young (7- to 8-week-old) male and female C57BL/6 mice (in approximate equal ratios) as well as NF-κB-GFP luciferase (NGL) reporter mice, and mice with conditional gain and loss of NF-κB. Specifically, to generate gain-of-function (GOF) or loss-of-function (LOF) NF-κB mice, IKK2ca (constitutive activated IKK2)[46,49] or IKK2flox mice[50] were respectively crossed with Villin-Cre mice and kept on a C57BL/6 background generating intestine epithelium conditional knock-in (cKI) and conditional knock-out (cKO) mice. Littermates were always used for control and treated groups. To induce colitis/IBD model, C57BL/6 mice (8 weeks old; $n = 6–8$ per treatment group) were given two intermittent cycles of 3 days of 3% DSS (Sigma, St. Louis, MO, USA) in their drinking water separated by 1 day of regular drinking and a final 2-day cycle of water at the end of the protocol. For administration of IKK2 inhibitors, DSS- or water-treated mice ($n = 5–9$) were intraperitoneally injected with a combination of two IKK2 inhibitor (ACHP 2 mg/kg and sc-514 30 mg/kg, MedChem Express, Monmouth Junction, NJ, USA) or vehicle (DMSO) daily, starting from 1 day before DSS treatment. At the end of the second cycle of treatment, mice were euthanized for analysis. To induce colitis in NF-κB reporter mice, DSS was added to the drinking water of NGL (NF-κB-GFP-luciferase) mice (The Jackson Laboratory, Bar Harbor, ME, USA) for 6 days, in which NF-κB signaling leads to the expression of a GFP/luciferase reporter. Collection of serum, cells, bones, intestines, and related analyses are described in detail in the sections that follow. Flow cytometry data were collected from pools of cells obtained from at least 4 mice per experiment and repeated 3 times. Serum cytokines were analyzed in individual mice ($n = 3–6$ per group). Approval for using animals was obtained from Washington University School of Medicine Institutional Animal Care and Use Committee in accordance with NIH guidelines before performing this study. Mice were housed at the Washington University School of Medicine barrier facility.

Statistical analysis

Results are presented as 1) mean ± SD; 2) fold change; and 3) representative images. Sample size ranged from 5 to 12 animals per group based on specific experiments. In cases where sufficient numbers of transgenic mice were not available

because of breeding limitations, 3 or 4 mice per group were conducted and pooled with repetition experiments to reach the desired number of mice per initial plan. In limited cases (2 cases), data were not collected from mice that succumb to death for unknown reasons. Within each experimental group, mice that were significantly smaller (>30% body weight) were excluded from the study to eliminate contribution of unknown factors to study results. During the duration of the study, only 2 mice were excluded. All experiments were repeated at least 3 times. Statistical analysis was performed using Prism 5.0 (GraphPad Software, GraphPad, La Jolla, CA, USA). The nonparametric Mann-Whitney test was applied for all statistical comparisons. Multiple treatments were analyzed by using one-way ANOVA followed by post hoc Newman-Keuls test of significance. Our goal is to reach 0.05 significance and an expected effect size of 25%. Standard deviation within groups is expected to not exceed 15%. Using a commercial power analysis tool (Rosner B, Fundamentals of biostatistics, 4th ed., section 8.10), we figured that for a desired difference 80% of the time, sample size is 6 mice per group. Where applicable, p values are indicated and consistently were $*p < 0.05$, $**p < 0.01$, and $***p < 0.001$ throughout the study. Specific p values that trended but were not significant were noted where applicable because of their overall importance.

μCT scan, bone histomorphometry, and histology

Femurs from experimental mice were harvested and fixed overnight in 10% formalin followed by washing with phosphate buffer saline (PBS) 3 times and transferred to 70% ethanol (v/v). Bones were scanned by Scanco Medical μCT systems (Scanco, Wayne, PA, USA) at the musculoskeletal core facility at Washington University (St. Louis, MO, USA). Briefly, images were scanned at a resolution of 20 μm, slice increment 20 μm, voltage 55 kV, current 145 μA, and exposure time of 200 ms. After scanning the whole bone, contours drawn from the growth plate toward trabecular regions of tibia of approximately 100 slices were analyzed, and 3D images were constructed. For bone histomorphometry analysis, fixed bones were decalcified by 14% EDTA for 14 days, followed by dehydration in graded alcohol before embedding in paraffin. Paraffin blocks were sectioned longitudinally. Five-micron sections were then stained with hematoxylin and eosin or tartrate-resistant acid phosphatase (TRAP) staining. For Trichrome's staining, intact (undecalcified) femurs were used for plastic sections after embedding in polymethyl methacrylate. For assessment of dynamic bone formation, mice were injected with calcein and alizarin (Sigma) 8 and 2 days, respectively, before euthanization. Sagittal histological bone sections were prepared, and the calcein bands were visualized by utilizing confocal laser microscopy. Single-labeled bone surface (sLS), double-labeled bone surface (dLS), and total bone surface (BS) were measured separately. Mineralizing surface per bone surface (MS/BS) was calculated as $(dLS + sLS/2)/BS^2$, and the mineral apposition rate (MAR) (μm/d) was measured as the distance between the parallel calcein labels.[51] Bone formation rate was calculated by multiplying MAR and MS/BS. For intestinal histology, colon and ileum from small intestine were fixed overnight in 10% formalin, followed by washing with PBS 3 times and transferred to 70% ethanol (v/v). Five microns of paraffin embedding sections were applied for H&E staining.

Isolation of bone marrow and flow cytometry

Single-cell suspensions from bone marrow were prepared by flushing the marrow out of femur and tibia. After red blood cell lysis, whole bone marrow cells were stained by Zombie UV dye to distinguish live/dead cells. Then bone marrow cells were resuspended in PBS with 2% FBS (FACS buffer), and further stained with biotin-conjugated lineage Ab cocktail (anti-B220, anti-CD3e, anti-Gr1, anti-Ter119). LSK^+ ($Lin^-Sca1^+ckit^+$) cells were stained with Ab cocktail (anti-Sca1 PerCP Cy5.5, anti-c-Kit APC eFluor 780, anti-CD34 FITC, and CD16/32 eFluor450). All FACS antibodies were purchased from either eBioscience, BioLegend (San Diego, CA, USA), or BD Bioscience (San Diego, CA, USA). After incubation on ice for 45 minutes, Ab-labeled cells were washed with FACS buffer and subjected to flow cytometric analysis (BD X-20). Data were analyzed with FlowJo software (TreeStar Inc., Ashland, OR, USA).

Cell culture

For osteoclastogenesis assay, 50 K whole bone marrow cells (WBMs) were counted and cultured in 96-well tissue culture plate with α-MEM (Invitrogen, Grand Island, NY, USA) containing 10% heat-inactivated FBS (Equitech-Bio, Kerrville, TX, USA), in the presence of macrophage colony-stimulating factor (M-CSF) (20 ng/mL) and receptor activator of NF-κB ligand (RANKL) (50 ng/mL). After 5 days, mature osteoclasts were fixed and stained for TRAP-positive multinuclear cells by using TRAP-leukocyte kit (Sigma). For assay of osteoclastogenesis-specific genes, 200 K of whole bone marrow free of red blood cells were cultured in osteoclastogenesis media for 3 days and cells were lysed for mRNA isolation. In case of osteoclastogenesis from IECs cocultured with WBMs, 20 K of sorted $CD326^+$ IECs were infected with lentivirus containing IKK2ca construct or control overnight (for 16 hours). Infected IECs were cocultured with 50 K of wild-type (WT)/WBMs in the absence or presence of permissive levels of RANKL (5 ng/mL) and M-CSF. After 5 days, cells were fixed and proceeded for TRAP staining to identify TRAP + MNCs formation. Additionally, infected IECs were also designed to be cocultured with sorted $CD3e^-CD19^-CD45^+$ ILC population for 48 hours to investigate ILC population by flow cytometry.

Quantification of mRNA levels by real-time PCR

Gene expression analyses were processed by lysing cells in Trizol reagent (Life Technologies). Total RNA was isolated using the PureLink RNA mini kit (Invitrogen). Complementary DNA was synthesized with High Capacity cDNA Reverse Transcription Kit (Applied Biosystems, Carlsbad, CA, USA). Gene expression was analyzed through real-time quantitative PCR reactions (qPCR) using the iQ SYBR Green Supermix (Bio-Rad, Hercules, CA, USA) and specific primers are listed in Supplemental Table S1. Target mRNA expression was calculated and normalized to the expression of the housekeeping gene Actin.

Enzyme-linked immunosorbent assay (ELISA)

Mice sera were collected from submandibular vein, and the serum inflammatory cytokine levels were detected using multiplex mouse cytokine kits (R&D Systems [Minneapolis, MN, USA] and Millipore [San Diego, CA, USA]). Serum cross-linked telopeptide of type I collagen (CTX-I) level was

quantified using the RatLaps EIA assay (Immunodiagnostic Systems, Boldon, UK). All procedures were performed according to their manufacturer's instructions.

Flow cytometry analysis of IKK2, pIKK2, and p-p65 in BM, spleen cells, MLNs, and IECs

Mice small intestines were cut open longitudinally, and Peyer's patches and fat were removed. Small intestines were cleaned and cut into pieces. Epithelial layers were extracted by incubation twice in HBSS containing 0.5 mM EDTA (Sigma) and 1 M HEPES (Sigma) for 20 minutes each at room temperature. The supernatant containing intestinal epithelial cells (IECs) were collected for flow cytometry analysis, and the remaining mucosa was further processed for lamina propria cell isolation. Pooled IECs were centrifuged with HBSS/PBS; the pellet was resuspended in PBS with 2% FBS and blocked with anti-CD16/32 antibody (BioLegend) for 30 minutes on ice. Cells were then stained with IEC markers anti-CD326 APC/Fire 750 (BioLegend) for 1 hour on ice. Bone marrow (BM) and spleen cells-derived $CD45^+$ lymphocytes, $CD4^+$ T cells, Th17 cells, and $CD11b^+$ macrophages were stained with Ab cocktail with anti-CD45 APC, anti-CD4 PE, and anti-RORγt PE-CF594. Mesenteric lymphoid cells (MLN)-derived T cells, B cells, and $CD45^+$ lymphocytes were stained with Ab cocktail with anti-CD3e PE-Cy7, anti-CD4 PE, anti-CD8 APC-Fire 750, anti-CD19 ef450, and anti-CD45 APC, respectively. For intracellular kinase staining, cells were fixed and permeabilized by Intracellular Fixation & Permeablization Buffer Set (eBioscience), followed by staining with antibodies against intracellular IKK2 (Novus Biologicals, Centennial, CO, USA), p-IKK2 (Cell Signaling, Danvers, MA, USA) or p-p65 (Cell Signaling) for 30 minutes on ice, and subsequently staining with FITC anti-rabbit IgG (BioLegend) or Alex 488 anti-mouse IgG (BioLegend) as conjugated second antibody for 1 hour. Stained cells were washed with FACS buffer and subjected to flow cytometric analysis (BD X-20). Data were analyzed with FlowJo software (TreeStar Inc.).

ILC isolation and flow cytometry

Lamina propria cells were isolated by digesting remaining mucosa after IEC extraction with collagenase VII (Sigma, St. Louis, MO) for 40 min at 37°C. After centrifuging at 2000 rpm for 10 minutes, mononuclear cells were isolated with 40% to 70% Percol gradient (Sigma) and washed twice with PBS. Pooled Lamina propria cells were resuspended in PBS with 2% FBS and blocked with anti-CD16/32 antibody (BioLegend) for 30 minutes on ice. ILCs were identified by staining with lineage Ab cocktail (anti-CD3e FITC, anti-CD19 FITC) and ILC1 Ab cocktail (anti-CD45 BV510, anti-NKp46 BV710, anti-NK1.1 PE), or ILC2 Ab cocktail (anti-CD45 BV510, anti-GATA3 Alex647), or ILC3 Ab cocktail (anti-CD45 BV510, anti-NKp46 BV710, anti-RORγt PE-CF594).[25,26] For intracellular cytokine and/or transcription factor staining, cells were fixed and permeablized by Intracellular Fixation & Permeablization Buffer Set (eBioscience), followed by staining with antibodies against intracellular cytokines or transcription factors (anti-TNFα ef450, anti-IFNγ BV650, anti-IL-17A BV786, anti-TGFβ PerCP-ef710, anti-GATA3 Alex647, and anti-RORγt PE-DZ594). All FACS antibodies were purchased from eBioscience, BioLegend, or BD Bioscience. Stained cells were washed with FACS buffer and subjected to flow cytometric analysis (BD X-20). Data were analyzed with FlowJo software (TreeStar Inc.). Gating strategy for each of the cell types is described in Supplemental Fig. S7*A–C*.

Results

Intestinal inflammation in DSS-colitis murine model leads to severe bone loss

To investigate the effect of colitis on bone, we utilized dextran sodium sulfate (DSS)-induced gut inflammation, a well-established murine IBD/colitis model.[52] In our study, 7- to 8-week-old C57BL/6 male and female mice were given two 3-day cycles of 3% (w/v) DSS in drinking water, an intermediate water-only day, and 2 days water as a final cycle before euthanization for a total period of 9 days. Administration of DSS induced colonic inflammation evident by histology and H&E staining of colon sections from DSS-treated mice, which displayed severe mucosal lesions manifested by alteration of epithelial structure, disruption of crypts structure, mucosal hyperplasia, shortening of intestine (Supplemental Fig. S1*A*, *B*), and significant loss of body weight compared with control (water)-treated mice (Supplemental Fig. S1*C*). To examine whether bone parameters were affected in DSS-treated mice, femoral trabecular bones were subjected to micro-CT analysis. As shown in Fig. 1*A*, a significant loss of trabecular bone structure was observed in femurs from DSS-treated mice compared with control mice, as reflected by reduced quantitative BV/TV (Fig. 1*B*), connective density (Supplemental Fig. S1*D*), trabecular number (Supplemental Fig. S1*E*), trabecular thickness (Supplemental Fig. S1*F*), and increased trabecular space (Supplemental Fig. S1*G*). Thus, chemical injury to the intestines causes significant bone loss.

Osteoclastogenesis is elevated and osteogenesis is impaired in DSS-induced colitis in mice

The significant bone loss we observed in DSS-colitis mice can be attributed to increased bone resorption, reduced bone formation, or a combination of both. Hence, we first tested the effect of DSS on osteoclasts and osteoblasts in vivo. To this end, femoral bone sections from control and DSS-treated mice were subjected to TRAP and trichrome staining. Bone formation rate (BFR) was determined by calcein and alizarin red double labeling in mice. TRAP staining of femur sections from DSS-treated mice showed an elevated osteoclast number in vivo (Fig. 1*C*, arrows pointing to red/purple-stained osteoclasts), which was further supported by exuberant ex vivo osteoclastogenic differentiation of bone marrow progenitors derived from DSS-treated mice compared with cells collected from vehicle counterparts (Fig. 1*D*, *E*; purple-stained cells). Consistently, expression of osteoclast-specific genes, such as TRAP, nuclear factor of activated T cells (NFATc1), and cathepsin K (CTSK), was higher in DSS-derived bone marrow cells (Fig. 1*F*). In addition, femoral trichrome, calcein/alizarin red double staining, and mRNA expression experiments showed reduction of mineralized compartments (indicated by reduced blue color), lower bone formation rate (Fig. 1*G–I*), and reduced expression of the osteogenic markers runt-related transcription factor 2 (RUNX2), collagen type I (Col1a), osteocalcin (OCN), and bone morphogenetic protein 2 (BMP2) (Supplemental Fig. S1*H*) in DSS-treated mice compared with control mice. These results indicate that DSS treatment generates a systemic response

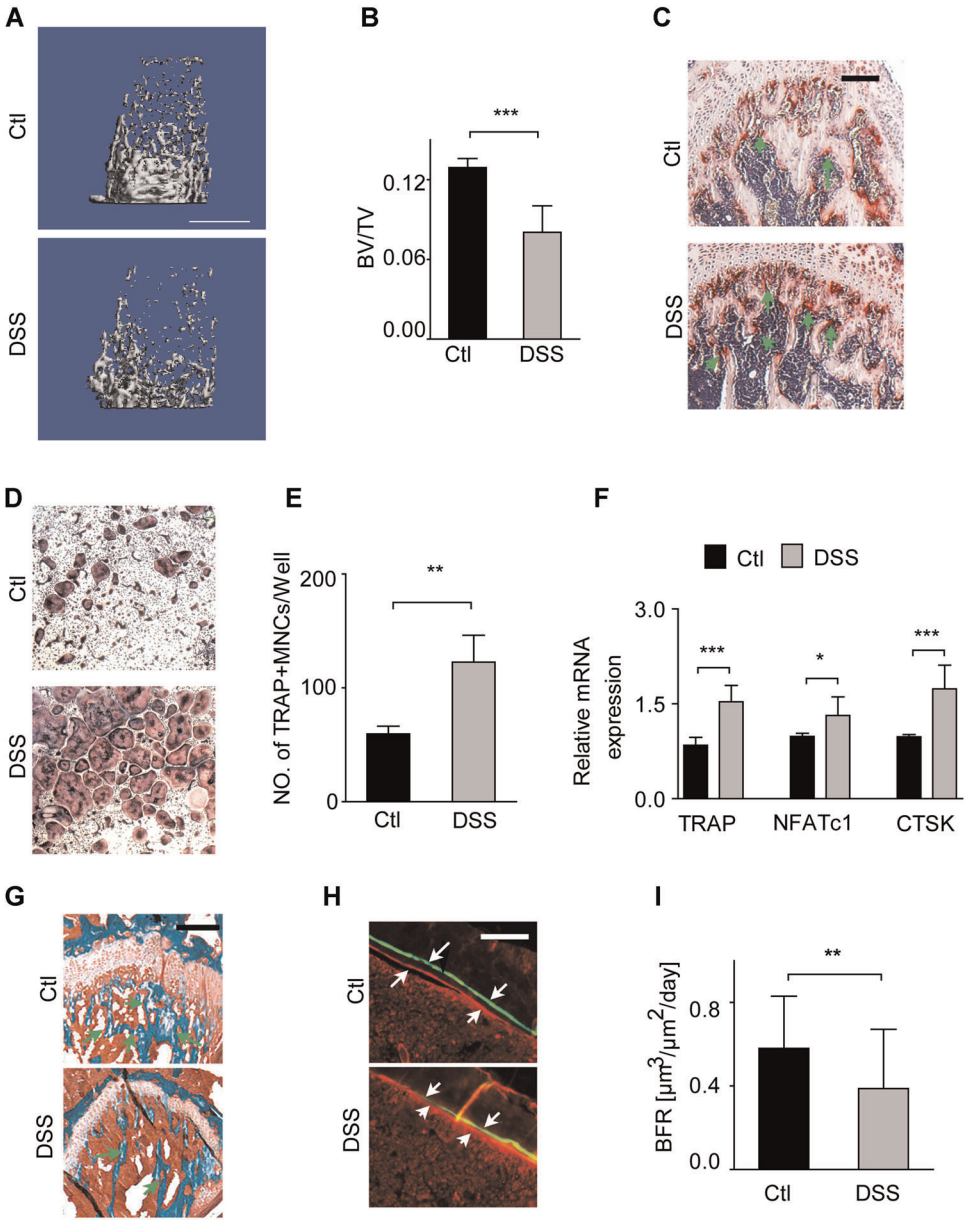

Fig. 1. DSS-induced colitis results in bone loss in mice. Water alone or water +3% (W/V) DSS was administered to 7- to 8-week-old WT mice ($n = 5$ per group, repeated 3 times) for 9 days intermittently. Mice were also injected, respectively, with calcein and alizarin 8 and 2 days before euthanization. At the end of the experiment, mice were euthanized and long bones were processed for analyses. (*A*) Micro-CT images of distal femur diaphysis (scale bar = 1 mm) and quantification of (*B*) bone volume (BV/TV). (*C*) TRAP staining of trabecular bone sections (scale bar = 100 μm). Separate bones were flushed and bone marrow progenitors were cultured for osteoclastogenesis (*D*, *E*), a portion of which was used to extract RNA and measure expression of osteoclast markers (*F*). Another set of long bones were processed for trichrome staining (*G*) and imaging to assess bone formation (*H*, *I*). (*G*, *H*) Scale bars = 100 μm. $^{*}p < 0.05$, $^{**}p < 0.01$, $^{***}p < 0.001$ [Color figure can be viewed at wileyonlinelibrary.com].

favoring osteoclast differentiation and, subsequently, bone resorption while inhibiting bone formation.

DSS/colitis-induced bone loss is associated with heightened inflammatory profile of IECs

Inflammation, characterized by overproduction of cytokines, is associated with increased bone resorption and decreased bone formation. The inflammatory cytokines produced during intestinal inflammation have also been reported in patients with bone loss.[53,54] Indeed, we measured copious amounts of inflammatory cytokines in the serum of DSS-treated mice, which included TNFα, IL-1β, MCP-1, IL-6, and RANKL, all of which contribute to inflammatory bone loss (Fig. 2*A*). We also found variably robust and some modest increases of circulating level of IL-17, IL-23, IL-10, G-CSF, GM-CSF, and DKK1 (Fig. 2*A*), cytokines that are notably involved in both bone and intestinal pathologies.[54,55] To elucidate the possible cellular source of these factors, we examined IECs, the gatekeepers of intestine mucosa. We find that IECs collected from the epithelial layer of

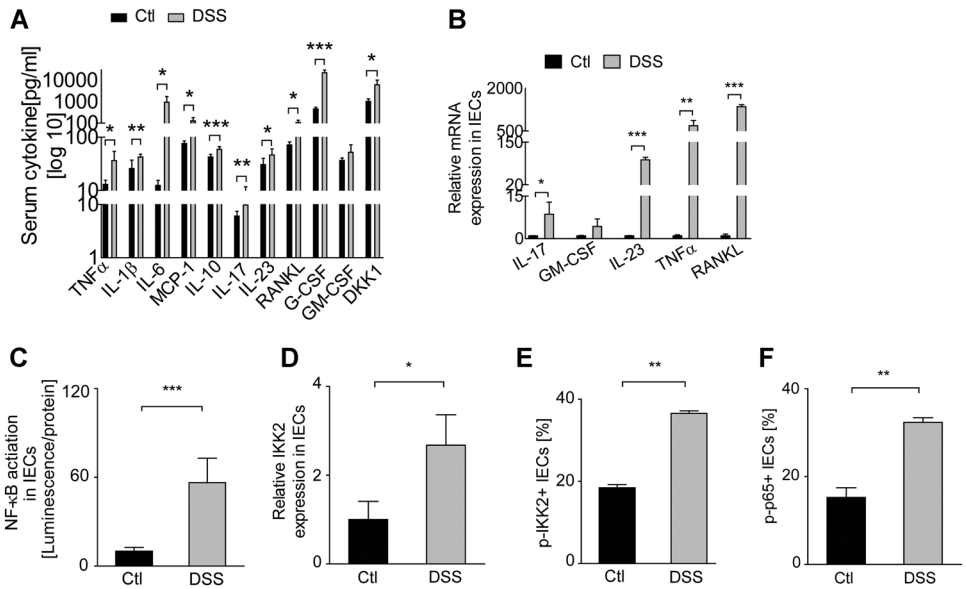

Fig. 2. Expression of inflammatory cytokines in serum and IECs derived from DSS-colitis is associated with robust NF-κB activation in IECs. (*A*) Serum and intestinal epithelial cells were collected from control ($n = 6$) and DSS-treated ($n = 6$) mice. Levels of serum cytokines were measured using Millipore Luminex ELISA. (*B*) Small intestine was processed to extract epithelial layer–derived IECs. Q-PCR was used to measure cytokine expression in IECs. (*C*) Luciferase assay was performed in IECs to measure NF-κB activation. The IECs were further sorted for $CD326^+$ cells and either lysed to measure mRNA expression of IKK2 (*D*) or stained to measure p-$IKK2^+CD326^+$ IECs (*E*) and p-$p65^+CD326^+$ IECs (*F*). The *y* axis in *A* and *B* is a log scale with breaks to accommodate presentation of low and high expressed cytokines in the same graph. $^*p < 0.05$, $^{**}p < 0.01$, $^{***}p < 0.001$.

DSS-treated mice express high levels of IL-23, IL-17, TNFα, GM-CSF, and RANKL mRNA compared with vehicle IECs (Fig. 2*B*).

DSS-induced gut inflammation activates NF-κB signaling in IECs

Because of its central role in inflammatory responses and cytokine secretion in various diseases including colitis,[3,56–60] we examined expression and activation of NF-κB in IECs. Using DSS-induced gut inflammation in NF-κB reporter mouse model, in which NF-κB signaling leads to the expression of a GFP-luciferase reporter, we show that overall NF-κB activation is significantly enhanced in IECs from DSS-treated reporter mice (Fig. 2*C*). To measure the intracellular NF-κB signaling pathway, expression and phosphorylation of IKK2 as well as phosphorylation of p65 were assessed in IECs by flow cytometry. DSS-induced colitis showed a greater percentage of IECs responding via increased IKK2 expression and phosphorylation (Fig. 2*D*, *E*) and p65 phosphorylation (Fig. 2*F*), indicative of NF-κB activation. These data suggest that activation of NF-κB signaling pathway in IECs mediates DSS-induced intestinal inflammation and is likely responsible for the abundant production of proinflammatory cytokines that ensues thereafter (Fig. 2*A*, *B*).

Genetic activation of NF-κB/IKK2 signaling in IECs mimics intestinal inflammation and induces bone loss

To directly test our proposition that NF-κB activation in IECs is sufficient to induce intestine inflammation and osteopenia, we generated a mouse model in which the constitutively active form of the principal NF-κB kinase IKK2 (IKK2ca thereafter) is specifically expressed in IECs. This task was accomplished by crossing mice carrying floxed IKK2ca in the pROSA locus[47] with Villin-cre mouse, resulting in conditional knock-in (cKI) and gain of function of IKK2ca in IECs (referred to as cKI mice). We reasoned that expression of IKK2ca in gut IECs could explain the pro-inflammatory skewing profile and the subsequent osteoclastic and bone loss phenotype observed in the DSS-intestine inflammation model.

Expression of IKK2 was analyzed in BM, spleen, gut residing mesenteric lymph node (MLN), $CD45^+$ lamino propria cells, as well as $CD326^+$ intestinal epithelial cells using flow cytometry. This analysis showed that IKK2 expression in CKI mice is specifically higher in $CD326^+$ IEC compared with other cell types, although there is also modest increased expression in $CD11b^+$ BMs (Supplemental Fig. S2*A*–*E*). In addition, cKI mice exhibited higher percentage of pIKK2 level in CD326-positve IECs cells (Supplemental Fig. S2*F*) compared with WT mice, an observation consistent with our previous findings in IECs derived from DSS-treated mice. cKI mice showed moderately reduced body weight (Supplemental Fig. S2*G*). H&E staining of colon and small intestine section showed that these transgenic mice developed spontaneous intestinal inflammation (thickening of membrane; arrow) with disorganized epithelial structure yet with no evidence of tissue erosion (Supplemental Fig. S2*H*). Notably, femoral micro-CT analysis results showed that cKI mice displayed significant trabecular bone loss (Fig. 3*A*–*E*) compared with their littermate wild-type (WT) mice. Consistently, immunohistochemistry showed abundant osteoclasts in trabecular bone sections of cKI mice (Fig. 3*F*; arrows pointing to red-stained osteoclasts). These findings were further supported by increased CTX values (biomarkers of bone resorption) in cKI mice (Fig. 3*G*) and by ex vivo findings

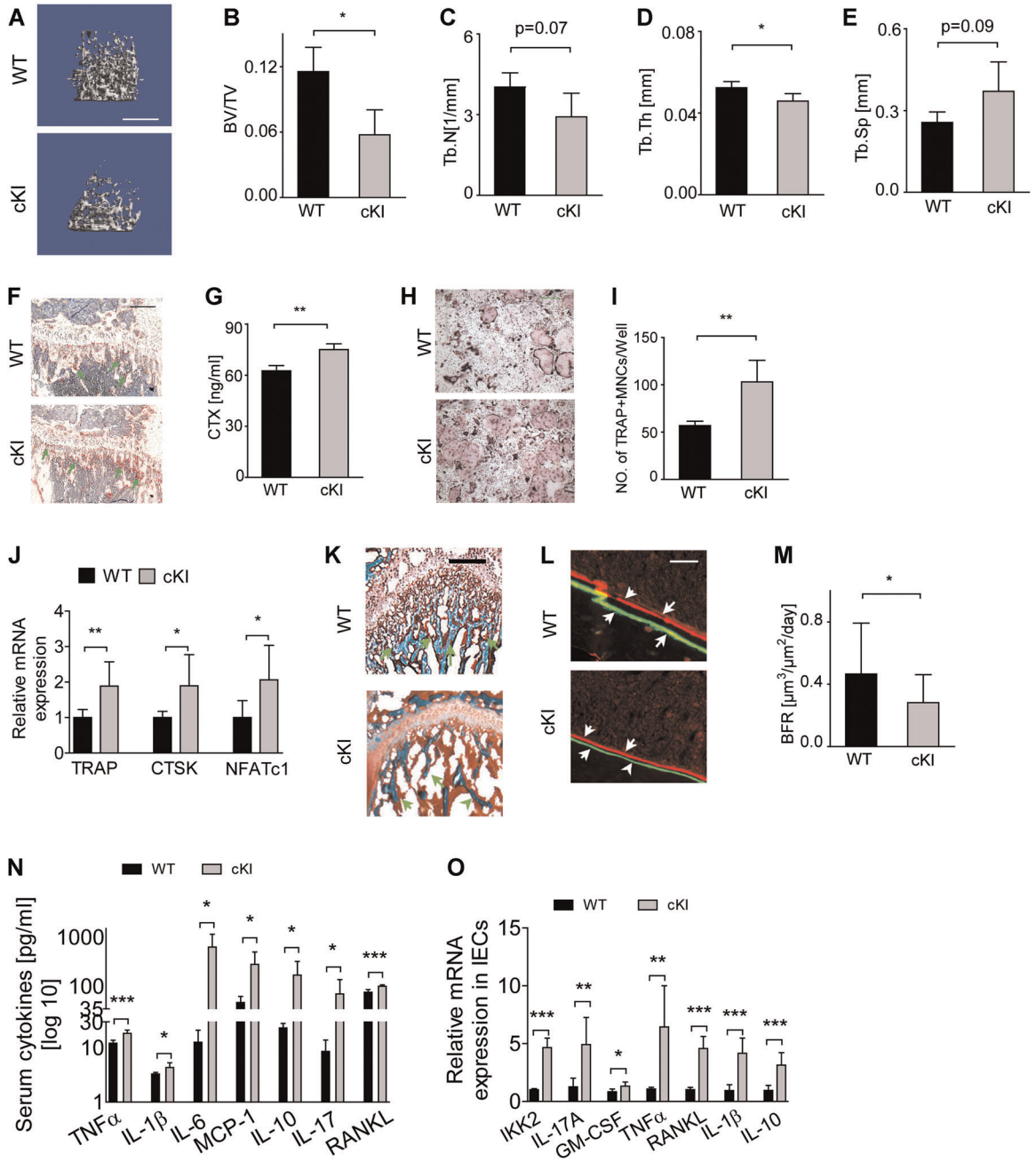

Fig. 3. Genetic activation of IKK2 in IEC mimics mild intestinal inflammation and induces bone loss. To analyze the direct role of NF-κB signaling in the progression of colitis, constitutively active IKK2 (IKK2ca)-floxed mice were crossed with the Villin-cre mice as described in Materials and Methods. At 8 weeks of age, the control (WT) ($n = 8$) and conditionally IKK2ca knock-in (cKI) mice ($n = 8$) were euthanized and were processed for different readouts. Long bones: µCT images of distal femur diaphysis (scale bar = 1 mm) (*A*) and quantification of bone volume (BV/TV) ($n = 4$) (*B*), trabecular number (Tb.N) (*C*), trabecular thickness (Tb.Th) (*D*) and trabecular separation (Tb.Sp) (*E*). After µCT, the bones were processed for histology (*F*) TRAP staining to visualize osteoclast per bone area (scale bar = 100 µm) and trichrome staining (scale bar = 100 µm) (*K*). CTX was measured in serum (*G*). Total bone marrow cells were isolated from WT and cKI mice and cultured in osteoclast differentiation media containing M-CSF and RANKL for 4 days and fixed, then TRAP-stained and counted (*H*, *I*). Cells were plated with M-CSF and RANKL followed by mRNA isolation and qPCR ($n = 8$) for OC genes TRAP, CTSK, and NFATc1 (*J*). The mice were also injected with consecutive labels of calcein and alizarin red (6 days apart) to measure bone formation rate (BFR) (*L*, *M*) ($n = 6$). Expression of different pro-inflammatory and anti-inflammatory cytokines in serum was measured using Millipore Luminex ELISA (*N*) ($n = 6$). mRNA expression of different cytokines was measured in isolated IECs using Q-PCR (*O*). The *y* axis in *N* is a log scale with breaks to accommodate presentation of low and high expressed cytokines in the same graph. $^{*}p < 0.05$, $^{**}p < 0.01$, $^{***}p < 0.001$ [Color figure can be viewed at wileyonlinelibrary.com].

demonstrating that bone marrow-derived myeloid cells collected from cKI mice generated far more osteoclasts in culture (Fig. 3*H*, *I*). Congruently, cKI-derived osteoclasts exhibited osteoclast gene expression profile much higher than cells derived from WT mice littermates (Fig. 3*J*). In addition, trichrome staining showed reduced mineralized compartments (Fig. 3*K*; reduced blue color) and reduced bone formation rate (Fig. 3*L*, *M*) in cKI mice. Analysis of femoral cortical bone showed that genetic activation of NF-κB/IKK2 signaling in IECs has a modest effect on cortical bone, which might be due to the short duration of experiments and the relative younger mice used for analysis (data not shown). Next, we attempted to verify whether the osteopenic phenotype in cKI mice was a consequence of highly exaggerated inflammatory cytokines. Similar to our observation in DSS-treated mice, levels of serum circulating cytokines in cKI mice showed elevated proinflammatory cytokines, with particular increased expression of TNFα, IL-6, IL-1β, MCP1, and IL-17A (Fig. 3*N*). Interestingly, we detected copious amounts of IL-10, a well-established antagonist of intestinal inflammation, and significant increase in RANKL levels, which is essential for osteoclastogenesis. To determine if these changes correlate with intrinsic effect of IKK2ca in IECs, we isolated these cells from the intestine epithelial layer of cKI mice and detected high expression of mRNA transcript for IKK2, IL-17A, IL-1β, TNFα, IL-10, RANKL, GM-CSF, and G-CSF among other cytokines (Fig. 3*O* and Supplemental Fig. S3), although a minor change of DKK1 level, pointing to a direct correlation between IEC cytokine expression profile and circulating cytokines. Collectively, these data provide direct evidence that conditional constitutive activation of IKK2 in the intestine mimics the osteopenic skeletal phenotype observed in DSS-treated mice, which supports a significant role of IKK2/NF-κB signaling in IECs as the culprit in IBD-bone loss axis.

Treatment with DSS or intrinsic expression of IKK2ca in IECs alters frequency of ILCs

It is believed that IEC-derived cytokines such as IL-23 and IL-17A facilitate cross-talk with innate lymphoid cells (ILCs), gut-residing cells that are considered professional cytokine-producing cells and crucial for mucosal homeostasis maintenance.[61] However, direct evidence that IECs regulate ILCs remains scarce. For this reason, we also examined frequency and cytokine expression by ILCs and observed increased frequency, in DSS-treated mice, of the pro-inflammatory ILC1(NK1.1$^+$) and ILC3(RORγt$^+$) cell populations (Fig. 4*A*), which also expressed high levels of inflammatory cytokines measured by cell fluorescence (Supplemental Fig. S4*A*, *B*). ILC2(GATA3$^+$) subsets appeared to be reduced after DSS treatment. Consistent with the notion that IECs regulate ILCs, as we suggested in the DSS-treated model, we identified enriched frequency of ILC3 and ILC1 populations within the CD45$^+$ lamina propria cells (Fig. 4*B* and Supplemental Fig. S4*C*) subsequent to knock-in of IKK2ca in IECs. We also determined enrichment of the corresponding signature intracellular cytokines, such as IFNγ, IL17A, and TNFα levels in ILC3 subsets (Fig. 4*C*). Interestingly, we also detected a drastic decrease in TGFβ in ILC3 (Fig. 4*C*), high levels of which have been shown to protect gut from injury by Smad-dependent suppression of NF-κB and proinflammatory cytokine production.[62] Collectively, although not conclusive, these results suggest that in response to chemical insult (DSS irritation), IECs produce a wide range of inflammatory cytokines, some of which, namely IL-23 and IL-17, are known to induce and activate ILCs.[63] Subsequently, ILC1 and ILC3 further produce cytokines and other factors that feed into and contribute to the rise of systemic inflammatory mediators.

Constitutive activation of IKK2ca in IECs alters frequency of osteoclast progenitors and IKK2 overexpressed IECs stimulates bone marrow-derived osteoclastogenesis

To further unravel the reasons for enhanced osteoclastogenesis, we examined the frequency of the myeloid progenitor population that gives rise to osteoclasts. Therefore, the LSK (Lin$^-$Sca$^+$cKit$^+$) population ratio, from which potent osteoclast progenitors and osteoclast founders arise, was determined in bone marrow from DSS-treated and cKI mice and their control counterparts. In both cases, the bone marrow of these mice exhibited enriched LSK population (Fig. 5*A*, *B*). This increased frequency together with the high propensity of these LSK cells to form more osteoclasts as we have shown previously[64] supports our hypothesis that the marrow microenvironment is sensitized by IEC and ILC-secreted cytokines and that NF-κB activity orchestrates this heightened response. Thus, IECs in the epithelial layer serve as sensors and guide inflammatory cytokines in an NF-κB-dependent manner to mount an ILC

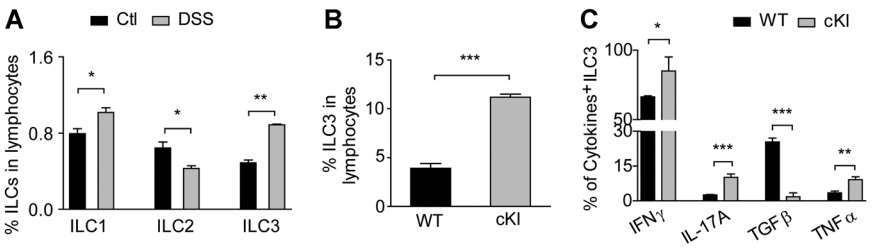

Fig. 4. Genetic activation of IKK2 in IECs leads to increased expression of inflammatory mediators in serum, IECs, and ILC3 cells. Small intestinal–derived lamina propria cells were collected from control ($n = 6$) and DSS-treated ($n = 6$) mice. Frequency of ILCs was measured using FACS analysis as described in Materials and Methods (*A*). Eight-week-old WT and cKI mice ($n = 6$ for each group) were euthanized and serum, bone marrow, and intestines were collected. Percent of ILC3 in total Lin$^-$CD45$^+$ lymphocyte population was measured by flow cytometry (*B* and Supplemental Fig. S7). Percent of cytokine-positive ILC3 was measured by flow cytometry of in-cell cytokine-specific fluorescence (*C* and Supplemental Fig. S7). $^*p < 0.05$, $^{**}p < 0.01$, $^{***}p < 0.001$.

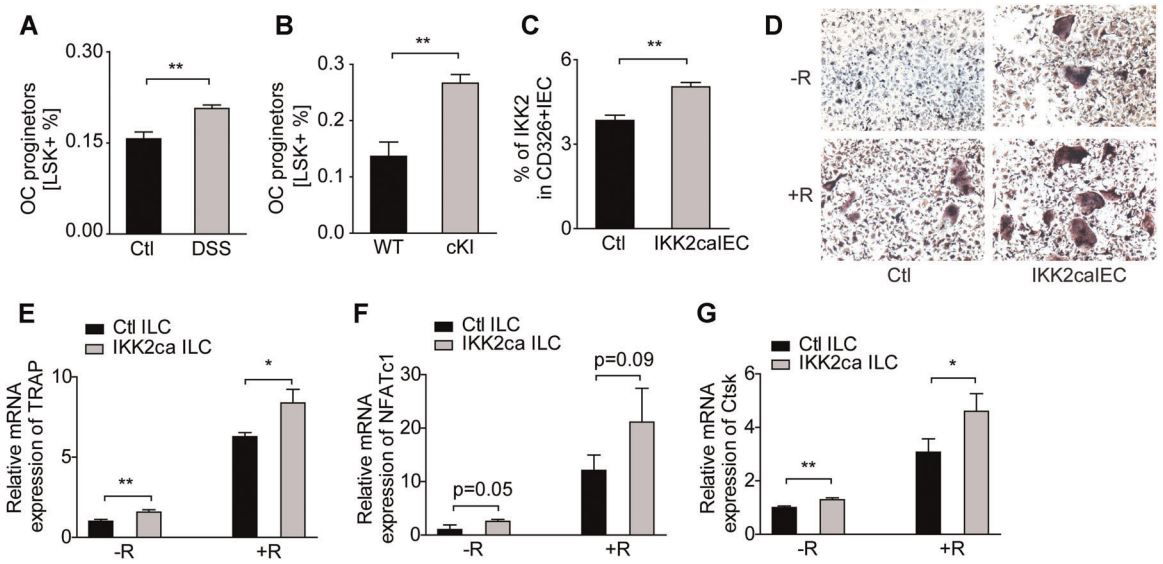

Fig. 5. cKI mice exhibit altered frequency of osteoclast progenitors, and IKK2 overexpressing IECs and ILCs stimulate bone marrow–derived osteoclastogenesis. Frequency of osteoclast progenitors (LSK cells) was measured by FACS analysis of marrow cells in DSS-treated mice (*A*), and cKI mice (*B*), with their corresponding control. An amount of 20 K of sorted CD326 + IECs were infected with control lentivirus (Ctl) or IKK2ca (IKK2calEC) overnight (for 16 hours), and efficiency of infection was evaluated by determination of % of IKK2 in CD326 + epithelial cells (*C*). Infected IECs were co-cultured with 50 K of WT/whole bone marrow in 96-well plates, in the absence (–R) or presence of permissive levels of RANKL (5 ng/mL) (+ R) and M-CSF (10 ng/mL). After 5 days, cells were fixed and proceeded for TRAP staining to identify TRAP + MNCs formation (*D*). An amount of 100 K of sorted $CD3^{-}CD19^{-}CD45^{+}$ILCs were infected with retrovirus containing control (Ctl) or IKK2ca construct (IKK2calLC) overnight (for 16 hours), and infected ILCs were co-cultured with 200 K of wild-type bone marrow cells, in the absence (–R) or presence of permissive levels of RANKL (5 ng/mL) (+ R) and M-CSF. Osteoclast-specific genes, such as TRAP, NFATc1, and Cathpsin K (CTSK), were determined in co-cultured cells after 5 days (*E–G*). $*p < 0.05$, $**p < 0.01$, $***p < 0.001$ [Color figure can be viewed at wileyonlinelibrary.com].

inflammatory response that culminates with increased frequency and potency of osteoclast progenitor population.

To further investigate whether IKK2-expressing intestinal epithelial cells are able to directly lead WBM-derived osteoclastogenesis, $CD326^{+}$ IECs were infected with lentivirus containing IKK2ca construct or control to generate stable pools of cells with increased expression of IKK2 (Fig. 5*C*). Co-culturing IECs with bone marrow cells showed that IECs infected with IKK2ca (IKK2calEC) are able to either directly induce WBM-derived osteoclastogenesis independent of exogenous RANKL (illustrated as –R) evident by presence of small TRAP + multinucleated osteoclasts (MNCs) (Fig. 5*D*) and also favor osteoclast differentiation in the presence of exogenously added permissive levels of RANKL (Fig. 5*D*, lower panels [+ R]). Since we suggest that inflammatory cytokine-producing ILCs are the major cells targeted by IKK2-intrinsic epithelial cells, to favor inflammatory bone environment, we also investigated direct effect of IKK2ca-infected epithelial cells on ILC population. Co-culture of IKK2calECs with ILCs ($CD3e^{-}CD19^{-}CD45^{+}$) induced modest propagation of ILC3 population (Supplemental Fig. S4*D*), pointing to direct polarization of the latter cells by IKK2ca-expressing IECs. Note that the amount of cytokines (ie, RANKL) produced by IECs or ILCs in vitro represent a small fraction of what these cell typically produce in vivo because of suboptimal microenvironment in vitro; hence, the reason behind conducting parallel experiment with permissive levels of RANKL. Next, we turn to examine whether IKK2ca-infected ILCs directly induce WBM-derived osteoclastogenesis. As shown in Fig. 5*E–G*, ILC cells infected with IKK2ca showed enhanced potential to increase WBM-derived osteoclastogenesis both in the presence or absence of RANKL stimulation, evident by increased expression of osteoclast-specific genes, such as TRAP, NFATc1, and CTSK. Indeed, our results showed that regardless of the experimental setting, IKK2-enriched IECs or ILCs are able to stimulate more osteoclastogenesis.

Conditional IKK2 deletion in IECs or pharmacological inhibition of IKK2 signaling normalizes changes in ILC populations, mitigates inflammatory burden, and protects DSS-treated mice from bone loss

Having established that constitutive activation of IKK2 in IECs is sufficient to mount an intestinal inflammatory response that leads to increased frequency of ILCs, secretion of pro-inflammatory cytokines, increased osteoclastogenesis, and subsequent bone loss, we surmised that deletion of IKK2 in IECs should abrogate the cellular changes and attenuate the inflammatory bone loss observed in DSS-treated mice. To this end, we generated one allele deletion of IKK2 in IECs by crossing floxed-IKK2 mice with villin-cre mice, which were then subjected to the DSS protocol. Examination of the bones by μCT of conditionally deleted IKK2 (cKO) mice revealed partial protection of the cKO from bone loss compared with significantly higher trabecular bone loss found in wild-type mice (Fig. 6*A*, *B* and Supplemental Fig. S5*A–D*), which was further supported by decreased osteoclast abundance in histological sections of DSS-treated cKO mice compared with DSS-treated WT mice (Supplemental Fig. S5*E*; arrow). More

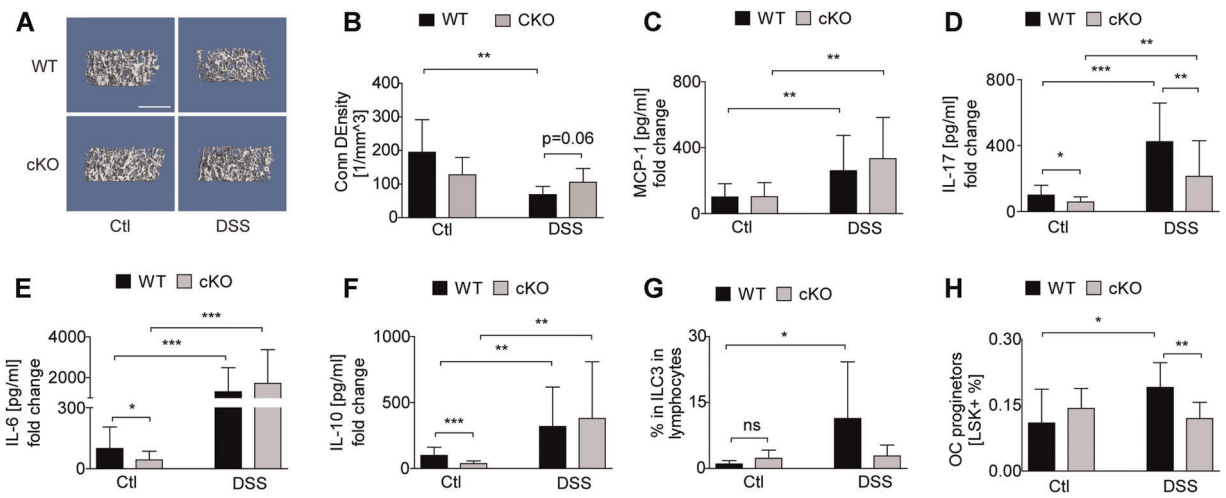

Fig. 6. IEC-specific inactivation of IKK2 significantly rescues DSS-induced bone loss. Serum, long bones, bone marrow, and intestines were collected from water or DSS-treated WT and IKK2 fl/fl:Villin cre- (cKO) mice. (*A*) μCT images of distal femur diaphysis (scale bar = 1 mm) and quantification of (*B*) connective density (WT/Ctl, $n = 6$; cKO/Ctl, $n = 6$; WT/DSS, $n = 7$; cKO/DSS, $n = 7$). (*C–F*) Serum levels of circulating cytokines measured by ELISA (WT/Ctl, $n = 7$; CKO/Ctl, $n = 6$; WT/DSS, $n = 8$; cKO/DSS, $n = 6$). (*G*) Percent of ILC3 cells in total lymphocytes collected from the lamina propria cells measured by FACS analysis (WT/Ctl, $n = 8$; cKO/Ctl, $n = 6$; WT/DSS, $n = 9$; cKO/DSS, $n = 7$). (*H*) Percent of LSK^+ OC progenitors in the marrow of different groups was measured using FACS analysis (WT/Ctl, $n = 9$; cKO/Ctl, $n = 8$; WT/DSS, $n = 10$; cKO/DSS, $n = 9$). $^*p < 0.05$, $^{**}p < 0.01$, $^{***}p < 0.001$ [Color figure can be viewed at wileyonlinelibrary.com].

importantly, deletion of IKK2 in IECs variably but significantly attenuated expression of the pro-inflammatory and osteoclastogenic cytokines IL-17A (Fig. 6*C–E*) and to a lesser degree of RANKL (Supplemental Fig. S5*F*), while increasing levels of the anti-inflammatory cytokine IL-10 (Fig. 6*F*) and IFNγ (Supplemental Fig. S5*G*) in cKO mice were sustained. Buttressing the key role of IKK2 in IEC and its secreted cytokines as gatekeepers of the intestine inflammatory response, we detected no increase in ILC3 frequency in DSS-treated IEC-cKO mice compared with the expected significant increase in DSS-treated WT mice (Fig. 6*G*). Similarly, frequency of LSKs was decreased in DSS-cKO mice compared with DSS-treated WT mice (Fig. 6*H*), which is consistent with protection of DSS-treated cKO mice from bone loss. Our results show a protective effect against DSS effect when IECs lack IKK2, as evident by significant and some modest decreases in levels of circulating cytokines, the latter which may be due to the systemic effect of DSS on other cell types. The variability we observed in detecting inconsistent amounts of cytokines, such as RANKL and IL-23, stems from the varying levels of IECs in vivo and dilution of the cytokines in the serum as opposed to consistently strong intrinsic expression by IECs. On the other hand, IL-10 levels increased more than 10-fold in DSS-treated cKO mice compared with corresponding controls, which may indicate a significant protective effect. However, the precise mechanism underpinning IL-10 changes remains to be explored.

To further probe the therapeutic value of our findings regarding the central role of IKK2/NF-κB in intestinal inflammation-mediated bone loss, we pharmacologically inhibited IKK2 activity by injecting DSS-treated mice with a combination of two IKK2-specific inhibitors (IKK2i), ACHP and sc-514. Gross examination (Supplemental Fig. S6*A*) and histological analysis of H&E-stained colon sections from DSS-treated mice (Supplemental Fig. S6*B*) showed that under IKK2i-treated conditions, significant reduction of inflammatory indices such as reduced intestine shortening, reduced tissue thickening, improved intestine crypt architecture, and viable cellularity were observed compared with vehicle-treated mice. This assessment was consistent with plummeted expression levels of inflammatory cytokines (Fig. 7*A–F* and Supplemental Fig. S6*C*, *D*), and reduced trend of ILC1 and ILC3 frequencies in DSS-treated mice exposed to IKK2 inhibitors compared with those treated with DSS alone (Fig. 7*G*, *H*). Most importantly, consistent with this overall reduced inflammatory burden in IKK2i-treated mice, μCT analysis of bone parameters showed that treatment of mice with IKK2 inhibitors significantly rescued bone loss induced in DSS-treated mice compared with vehicle-treated mice (Fig. 7*I*) evident by improved trabecular BV/TV (Fig. 7*J*) and other bone parameters such as connective tissue density, trabecular number, as well as reduced trabecular space (Supplemental Fig. S6*E–H*). Histological analysis of TRAP-stained bone sections further confirmed that IKK2i reduced osteoclasts in DSS + IKK2i-treated animals compared with those treated with DSS alone (Fig. 7*K*). These observations were further substantiated by decreased levels of cross-links (CTX) that reflect bone resorptive activity of osteoclasts in vivo in the IKK2i-treated mice (Supplemental Fig. S6*I*). Taken together, our findings show that intrinsic expression of active IKK2 elicits inflammatory effects in IECs and that IEC-specific deletion or systemic inhibition of this kinase is beneficial to reduce levels of inflammatory cytokines and cells in the lamina propria and alleviates bone loss associated with gut inflammation.

Discussion

Bone loss has been linked to chronic gut inflammation. Despite extensive research, the mechanistic underpinning of this health

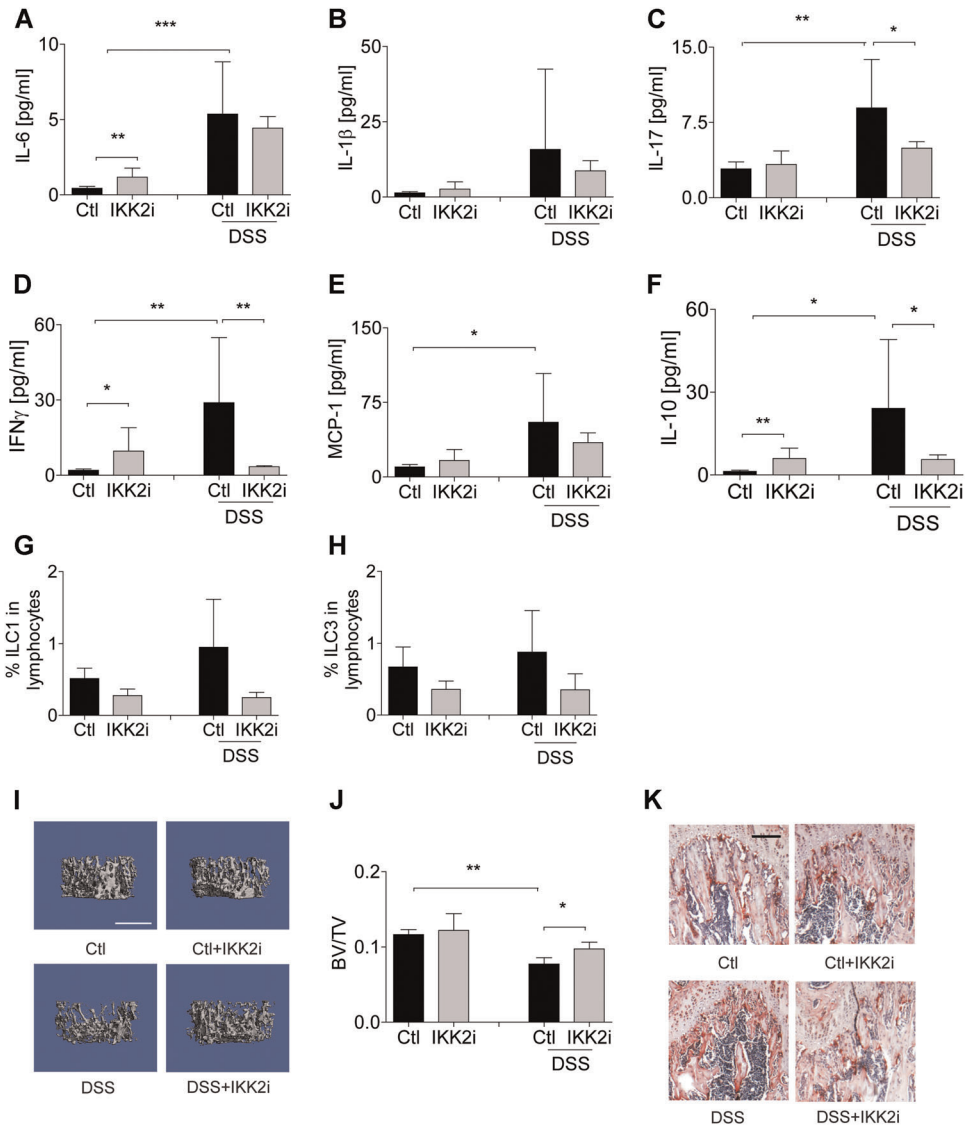

Fig. 7. Pharmacological inhibition of IKK2 partially but significantly rescues DSS-induced bone loss. Serum, bones, bone marrow, and intestines were collected from vehicle or IKK2 inhibitor–injected (9 days) control and DSS-treated mice (Ctl, $n = 3$; Ctl + IKK2i, $n = 4$; DSS, $n = 3$; DSS + IKK2i, $n = 4$; repeated 3 times). Serum levels of pro- and anti-inflammatory cytokines were measured using ELISA (*A–F*). (*G*, *H*) Percent of ILC1 and ILC3 cells in total lymphocytes was measured by FACS analysis (Ctl, $n = 3$; Ctl + IKK2i, $n = 4$; DSS, $n = 3$; DSS + IKK2i, $n = 4$). μCT images (scale bar = 1 mm) of distal femur diaphysis (*I*) and quantification of bone volume (BV/TV) (*J*) (Ctl, $n = 3$; Ctl + IKK2i, $n = 4$; DSS, $n = 3$; DSS + IKK2i, $n = 4$). Long bones were fixed and processed for immunohistochemistry using TRAP staining (*K*; scale bar = 100 μm) to detect osteoclasts (red/purple color). $^{*}p < 0.05$, $^{**}p < 0.01$, $^{***}p < 0.001$ [Color figure can be viewed at wileyonlinelibrary.com].

predicament remains elusive. In this study, we identified IKK2 in IECs as a primary mediator of this inflammatory response. cKI mice showed mild intestinal inflammation evident by moderately reduced body weight (Supplemental Fig. S2*G*), relative disorganized colon epithelial structure (Supplemental Fig. S2*H*) not affecting colon length (data not shown), and no evidence of erosion compared with DSS colitis-induced mice (Supplemental Fig. S1*A–C*). Hence, we took advantage of the mild pathology of IKK2ca IBD-like model to interrogate the mechanistic aspects sparing the confounding epithelial erosive aspects associated with DSS-IBD. Stimulated IECs trigger changes in pro-inflammatory ILC1 and ILC3 cells, which, similar to IECs, produce ample inflammatory cytokines and growth factors in response to mucosal antigen-presenting cells, evident by expression of IL-1β, IL-6, IL-23, IL-17A, and IFNγ, as well as in response to local cytokine milieu. This leads to increased frequency of ILCs locally, which is consistent with previous findings that described increased ILCs in the gut and in gut-associated lymph nodes during IBD (summarized in Buela and colleagues[65]). Local changes in IECs and ILCs appear to summon remote systemic effects including increased frequency of marrow myeloid cells, the precursor cells for osteoclasts, presumably due to abundance of circulating cytokines. Indeed, our novel observation that IECs, and

potentially ILCs, express RANKL, TNFα, and IL-17 directly support the role of these cells as regulators of bone cells, as they both support osteoclastogenesis (Fig. 5). To our knowledge, these findings are the first to establish the role of IECs and ILCs in bone homeostasis and pathogenesis.

The highlight of our studies is establishing the direct and critical role played by NF-κB at the apex of gut inflammation, connecting gut and bone pathogeneses. Specifically, using cell-specific genetic approach, we provide unequivocal evidence that conditional expression or deletion of IKK2 in IECs modulates intestine-residing immune cells, namely ILCs, regulates expression of inflammatory and osteoclastogenic factors, and modulates bone homeostasis. Specifically, gain-of-function IKK2ca in IECs mimics the DSS irritant effect evidenced by secretion of TNFα, IL-1β, IL-6, MCP-1, IL-17, and RANKL. Consistently, deletion of IKK2 in IECs dwindled secretion of these cytokines in response to chemical irritants. The role of NF-κB as a principal effector of gut inflammation was validated in earlier studies,[56,59,66,67] in which it was demonstrated that IKK2 and IKKγ/NEMO directly regulate intestine immunity and their dysregulation through activation or genetic ablation, respectively, contributes directly to the pathogenesis of IBD in mice. However, it is important to note that whereas exacerbated activation of NF-κB under inflammatory conditions is pathogenic and harmful, baseline activity of NF-κB is important for the maintenance of physiological immune homeostasis, which was predominantly observed in epithelial cells. It is for this reason that we employed an IKK2 haplo-insufficient approach. In this regard, and consistent with previous studies,[66] we observed that complete deletion of both IKK2 alleles in IECs results in destructive effects, whereas deletion of one allele elicits the opposite result, namely, lowers the inflammatory burden and protects IECs, resulting in healthy intact intestine crypts that are less responsive to chemical insults. On the other hand, we also noticed the expression of constitutively active IKK2 in IECs, while mounting robust inflammatory response, did not affect the integrity of the intestine epithelial layer and did not lead to tissue destructive effects. This latter finding is also supported by earlier observation.[68] The data depicted in this body of work suggests that inflammatory IECs produce a wide range of cytokines including RANKL, TNFα, IL-17, IL-1β, IL-6, and other osteotropic cytokines and growth factors. Cellular analysis shows that frequency of the potent marrow-derived osteoclast progenitors LSK population is increased under gut inflammatory conditions. These cells are sensitized and readily differentiate into osteoclasts in the presence of RANKL, TNFα, IL-17, and the various osteoclastogenic cytokines mentioned earlier. This circumstance is consistent with earlier findings in which we show that systemic inflammation in scurfy (*foxp3* mutant) mice leads to dramatic osteopenia due to expression of copious amounts of cytokines, skewing, and sensitization of the bone marrow LSK population,[69] resulting in exacerbated osteoclastogenesis. More to this point, we observed significant reduction of TGFβ in ILCs derived from cKI mice, while serum levels of IL-10 remained high. TGFβ and IL-10 are anti-inflammatory factors typically produced by regulatory T cells (T_{REGS})[70] and as our data suggest by ILC cells. TGFβ has also been shown to protect from gut injury by inhibiting NF-κB and pro-inflammatory cytokine production in a Smad-dependent manner.[62] Therefore, it is reasonable that reduced TGFβ levels, which is also essential for activating T_{REG} cells, may contribute to decline in the anti-osteoclastogenic activity and elevated levels of pro-inflammatory and pro-osteoclastogenic factors by these lymphocytes. On the other hand, elevated levels of IL-10 may reflect a feedback mechanism to counter the robust inflammatory response.

Individual therapies such as neutralization of IL-17, blocking IL-13, or IP-10 have failed to produce protective effect in ulcerative colitis patients, suggesting that greater cytokine redundancy exists in colitis.[71] This is especially detrimental in the case of the bone loss comorbidity due to its sensitivity to most inflammatory cytokines, rendering strategies to target individual cytokines obsolete. In contrast, targeting NF-κB, which resides at the apex and mediates the actions of most inflammatory cytokines, encompasses greater breadth and explains the therapeutic efficacy we demonstrate in our study. Caution should be taken, however, to avoid complete shutdown of NF-κB signaling, baseline activity of which is essential for cell survival and cellular homeostasis.

It has been suggested that the IL23/IL17A inflammatory axis governs the cross-talk between innate and adaptive immunity during gut inflammation and induces ILCs. In this regard, Buonocore and colleagues[72] identified ILCs as being responsible for intestinal inflammation through secretion of IL-17A or IFN-γ and recruitment of other cells. This process includes recruitment of adaptive immune T-cell populations evident by rising levels of IL-12, IFN-γ, and IL-2. Altogether, it is likely that the initial trigger of IECs by irritants leads to NF-κB-dependent production of first-tier inflammatory cytokines, which subsequently recruit and activate innate and adaptive immune cells that exacerbate the inflammatory response through production of excessive amounts of cytokines.

We have observed cytokine variability among different models that we believe reflect fundamental differences due to the nature of immune response in DSS-induced model compared with the tissue-restricted IKK2ca-elicited model. Specifically, it is well documented that DSS disrupts the intestinal barrier function and summons a wider-range immune response compared with cKI mice. Therefore, targeting NF-κB in the IECs, while appearing effective in reducing the inflammatory burden and bone loss, is not expected to reverse the entire destructive effects of DSS. Hence, the relative intestine architectural protection that we observed after deletion versus inhibition of IKK2 in the two models must reflect a consequence of the decreased abundance of inflammatory cytokines and immune cells that contribute to and exacerbate tissue damage in each model. Although deletion of IKK2 in IECs is not expected to attenuate the inflammatory response of other gut-residing immune cells in response to DSS, systemic inhibition of IKK2 alters the overall inflammatory response, albeit in a non-cell-specific manner.

Our study has some limitations. Gut inflammation causes dramatic changes in the microbiota, whose impact on skeletal health has been recently recognized.[73] Although it is likely that such changes occur in our IKK2 gain- and loss-of-function models, studying this aspect deserves an independent study. We have also limited the scope of our studies to the function of IECs and ILCs. We recognize the robust research performed over the past decades defining the contribution of various innate and adaptive immune cells during gut inflammation. Our focus on IECs and ILCs emanates from our belief that these cells coordinate the mucosal immune response and regulate innate and adaptive cell responses. Future studies will explore the specific impact of NF-κB manipulations on other immune cells and its relevance to skeletal homeostasis.

Finally, despite our observation that gut inflammation affects both bone resorption and bone formation, we have focused on

characterizing the mechanism underpinning bone resorption. This choice was based on our belief that inhibiting bone resorption will provide significant bone protection outcome due to the heightened bone breakdown we observed. This choice does not detract from the likely significant effect of gut inflammation on inhibiting bone formation. In fact, our data show that levels of bone inhibitors such as the Wnt antagonist DKK1[74,75] and G-CSF[76] are elevated in the serum of mice with gut inflammation. Although studies targeting these molecules have been described, future mechanistic studies are required to unravel the full spectrum of their negative effect on the skeleton.

Disclosures

All authors state that they have no conflicts of interest.

Acknowledgments

This work was supported by NIH/NIAMS R01-AR049192, R01-AR054326, and R01-AR072623 (to YA), Biomedical grant #86200 from Shriners Hospital for Children (to YA), P30 AR057235 NIH Core Center for Musculoskeletal Biology and Medicine (to YA), and NIH/NIAMS R01-AR064755 and R01-AR068972 (to GM).

Authors' roles: YA conceived, developed, and supervised the project and finalized the manuscript. KK performed experiments, presented and analyzed data, participated in development of the project, and significantly contributed to manuscript writing. GS, MA, and TC participated in performing experiments and data analysis. GM participated in experimental design, data analysis, and manuscript preparation.

References

1. Tanaka Y, Nakayamada S, Okada Y. Osteoblasts and osteoclasts in bone remodeling and inflammation. Curr Drug Targets Inflamm Allergy. 2005;4:325–8.
2. Bianchi ML. Inflammatory bowel diseases, celiac disease, and bone. Arch Biochem Biophys. 2010;503:54–65.
3. Abu-Amer Y. Inflammation, cancer, and bone loss. Curr Opin Pharmacol. 2009;9:427–33.
4. Cheung WW, Zhan JY, Paik KH, Mak RH. The impact of inflammation on bone mass in children. Pediatr Nephrol. 2010;1–10.
5. Cochran DL. Inflammation and bone loss in periodontal disease. J Periodontol. 2008;79:1569–76.
6. Mundy GR. Osteoporosis and inflammation. Nutr Rev. 2007;65:S147–51.
7. Tilg H, Moschen AR, Kaser A, Pines A, Dotan I. Gut, inflammation and osteoporosis: basic and clinical concepts. Gut. 2008;57:684–94.
8. Schuettpelz LG, Link DC. Regulation of hematopoietic stem cell activity by inflammation. Front Immunol. 2013;4:204.
9. McInnes IB, Schett G. Cytokines in the pathogenesis of rheumatoid arthritis. Nat Rev Immunol. 2007;7:429–42.
10. Horwood N. Lymphocyte-derived cytokines in inflammatory arthritis. Autoimmunity. 2008;41:230–8.
11. Ghishan FK, Kiela PR. Advances in the understanding of mineral and bone metabolism in inflammatory bowel diseases. Am J Physiol Gastrointest Liver Physiol. 2011;300:G191–G201.
12. Diarra D, Stolina M, Polzer K, et al. Dickkopf-1 is a master regulator of joint remodeling. Nat Med. 2007;13:156–63.
13. Heiland GR, Zwerina K, Baum W, et al. Neutralisation of Dkk-1 protects from systemic bone loss during inflammation and reduces sclerostin expression. Ann Rheum Dis. 2010;69:2152–9.
14. Ke HZ, Richards WG, Li X, Ominsky MS. Sclerostin and Dickkopf-1 as therapeutic targets in bone diseases. Endocr Rev. 2012;33:747–83.
15. Sarahrudi K, Thomas A, Albrecht C, Aharinejad S. Strongly enhanced levels of sclerostin during human fracture healing. J Orthop Res. 2012;30:1549–55.
16. Hamdani G, Gabet Y, Rachmilewitz D, Karmeli F, Bab I, Dresner-Pollak R. Dextran sodium sulfate-induced colitis causes rapid bone loss in mice. Bone. 2008;43:945–50.
17. Haynes DR. Bone lysis and inflammation. Inflamm Res. 2004;53: 596–600.
18. Romas E, Gillespie MT. Inflammation-induced bone loss: can it be prevented? Rheum Dis Clin N Am. 2006;32:759–73.
19. Sweeney SE, Firestein GS. Rheumatoid arthritis: regulation of synovial inflammation. Int J Biochem Cell Biol. 2004;36:372–8.
20. Walsh NC, Crotti TN, Goldring SR, Gravallese EM. Rheumatic diseases: the effects of inflammation on bone. Immunol Rev. 2005;208:228–51.
21. Cassinotti A, Sarzi-Puttini P, Fichera M, Shoenfeld Y, deFranchis R, Ardizzone S. Immunity, autoimmunity and inflammatory bowel disease. Autoimmun Rev. 2014;13:1–2.
22. Strober W, Fuss I, Mannon P. The fundamental basis of inflammatory bowel disease. J Clin Invest. 2007;117:514–21.
23. Andrews C, McLean MH, Durum SK. Cytokine tuning of intestinal epithelial function. Front Immunol. 2018;9:1270.
24. Geremia A, Biancheri P, Allan P, Corazza GR, Di Sabatino A. Innate and adaptive immunity in inflammatory bowel disease. Autoimmun Rev. 2014;13:3–10.
25. Sonnenberg GF, Artis D. Innate lymphoid cells in the initiation, regulation and resolution of inflammation. Nat Med. 2015;21:698–708.
26. Vivier E, Artis D, Colonna M, et al. Innate lymphoid cells: 10 years on. Cell. 2018;174:1054–66.
27. Monteleone I, Sarra M, Pallone F, Monteleone G. Th17-related cytokines in inflammatory bowel diseases: friends or foes? Curr Mol Med. 2012;12:592–7.
28. DeNitto D, Sarra M, Cupi ML, Pallone F, Monteleone G. Targeting IL-23 and Th17-cytokines in inflammatory bowel diseases. Curr Pharm Des. 2010;16:3656–60.
29. Geremia A, Jewell DP. The IL-23/IL-17 pathway in inflammatory bowel disease. Expert Rev Gastroenterol Hepatol. 2012;6:223–37.
30. Geremia A, Arancibia-Carcamo CV, Fleming MP, et al. IL-23-responsive innate lymphoid cells are increased in inflammatory bowel disease. J Exp Med. 2011;208:1127–33.
31. Mei J, Liu Y, Dai N, et al. Cxcr2 and Cxcl5 regulate the IL-17/G-CSF axis and neutrophil homeostasis in mice. J Clin Invest. 2012;122:974–86.
32. Gyires K, Toth EV, Zadori SZ. Gut inflammation: current update on pathophysiology, molecular mechanism and pharmacological treatment modalities. Curr Pharm Des. 2014;20:1063–81.
33. Fukuzawa H, Sawada M, Kayahara T, et al. Identification of GM-CSF in Paneth cells using single-cell RT-PCR. Biochem Biophys Res Commun. 2003;312:897–902.
34. Ito R, Kita M, Shin-Ya M, et al. Involvement of IL-17A in the pathogenesis of DSS-induced colitis in mice. Biochem Biophys Res Commun. 2008;377:12–16.
35. Siebenlist U, Franzoso G. Structure, regulation and function of NF-kB. Proc Natl Acad Sci U S A. 2001;89:4333–7.
36. Tak P, Firestein G. NF-kB: a key role in inflammatory diseases. J Clin Invest. 2001;107:7–11.
37. Ting AY, Endy D. Signal transduction: decoding NF-kB signaling. Science. 2002;298:1189–90.
38. Yamamoto Y, Gaynor R. Therapeutic potential of inhibition of the NF-kB pathway in the treatment of inflammation and cancer. J Clin Invest. 2001;107:135–42.
39. Hayden MS, Ghosh S. Signaling to NF-kB. Genes Dev. 2004;18:2195–224.
40. Abu-Amer Y, Faccio R. Therapeutic approaches in bone pathogeneses: targeting the IKK/NF-kB axis. Future. Medicine. 2006;1:133–46.

41. Hacker H, Karin M. Regulation and function of IKK and IKK-related kinases. Sci STKE. 2006;357:re13.
42. Karin M, Yamamoto Y, Wang M. The IKK NF-kB system: a treasure trove for drug development. Nat Rev. 2004;3:17–26.
43. Ruocco MG, Karin M. IKK{beta} as a target for treatment of inflammation induced bone loss. Ann Rheum Dis. 2005;64(Suppl 4):iv81–5.
44. Ruocco MG, Maeda S, Park JM, et al. IkB kinase-beta, but not IKK-alpha, is a critical mediator of osteoclast survival and is required for inflammation-induced bone loss. J Exp Med. 2005;201:1677–87.
45. Schopf L, Savinainen A, Anderson K, et al. IKK beta inhibition protects against bone and cartilage destruction in a rat model of rheumatoid arthritis. Arthritis Rheum. 2006;54:3163–73.
46. Otero JE, Chen T, Zhang K, Abu-Amer Y. Constitutively active canonical NF-kappaB pathway induces severe bone loss in mice. PLoS ONE. 2012;7:e38694.
47. Otero JE, Dai S, Alhawagri MA, Darwech I, Abu-Amer Y. IKKbeta activation is sufficient for RANK-independent osteoclast differentiation and osteolysis. J Bone Miner Res. 2010;25:1282–94.
48. Sasaki Y, Derudder E, Hobeika E, et al. Canonical NF-[kappa]B activity, dispensable for B cell development, replaces BAFF-receptor signals and promotes B cell proliferation upon activation. Immunity. 2006;24:729–39.
49. Swarnkar G, Zhang K, Mbalaviele G, Long F, Abu-Amer Y. Constitutive activation of IKK2/NF-κB impairs osteogenesis and skeletal development. PLoS ONE. 2014;9:e91421.
50. Otero JE, Dai S, Foglia D, et al. Defective osteoclastogenesis by IKKbeta-null precursors is a result of receptor activator of NF-kappaB ligand (RANKL)-induced JNK-dependent apoptosis and impaired differentiation. J Biol Chem. 2008;283:24546–53.
51. Nagao M, Feinstein TN, Ezura Y, et al. Sympathetic control of bone mass regulated by osteopontin. Proc Natl Acad Sci U S A. 2011;108:17767–72.
52. Eichele DD, Kharbanda KK. Dextran sodium sulfate colitis murine model: an indispensable tool for advancing our understanding of inflammatory bowel diseases pathogenesis. World J Gastroenterol. 2017;23:6016–29.
53. Rios-Arce ND, Collins FL, Schepper JD, et al. Epithelial barrier function in gut-bone signaling. Adv Exp Med Biol. 2017;1033:151–83.
54. Collins FL, Schepper JD, Rios-Arce ND, et al. Immunology of gut-bone signaling. Adv Exp Med Biol. 2017;1033:59–94.
55. Takayanagi H. Osteoimmunology: shared mechanisms and crosstalk between the immune and bone systems. Nat Rev Immunol. 2007;7:292–304.
56. Wullaert A, Bonnet MC, Pasparakis M. NF-kB in the regulation of epithelial homeostasis and inflammation. Cell Res. 2011;21:146–58.
57. Yan YX, Shao MJ, Qi Q, et al. Artemisinin analogue SM934 ameliorates DSS-induced mouse ulcerative colitis via suppressing neutrophils and macrophages. Acta Pharmacol Sin. 2018;39:1633–44.
58. Li H, Liang Y, Lai X, Wang W, Zhang J, Chen S. Genetic deletion of Fbw7 in the mouse intestinal epithelium aggravated dextran sodium sulfate-induced colitis by modulating the inflammatory response of NF-kappaB pathway. Biochem Biophys Res Commun. 2018;498:869–76.
59. Guma M, Stepniak D, Shaked H, et al. Constitutive intestinal NF-kappaB does not trigger destructive inflammation unless accompanied by MAPK activation. J Exp Med. 2011;208:1889–900.
60. Spehlmann ME, Eckmann L. Nuclear factor-kappa B in intestinal protection and destruction. Curr Opin Gastroenterol. 2009;25:92–9.
61. Mortha A, Burrows K. Cytokine networks between innate lymphoid cells and myeloid cells. Front Immunol. 2018;9:191.
62. Shiou SR, Yu Y, Guo Y, et al. Oral administration of transforming growth factor-beta1 (TGF-beta1) protects the immature gut from injury via Smad protein-dependent suppression of epithelial nuclear factor kappaB (NF-kappaB) signaling and proinflammatory cytokine production. J Biol Chem. 2013;288:34757–66.
63. Gaffen SL, Jain R, Garg AV, Cua DJ. The IL-23-IL-17 immune axis: from mechanisms to therapeutic testing. Nat Rev Immunol. 2014;14:585–600.
64. Chen TH, Swarnkar G, Mbalaviele G, Abu-Amer Y. Myeloid lineage skewing due to exacerbated NF-kappaB signaling facilitates osteopenia in Scurfy mice. Cell Death Dis. 2015;6:e1723.
65. Buela KA, Omenetti S, Pizarro TT. Cross-talk between type 3 innate lymphoid cells and the gut microbiota in inflammatory bowel disease. Curr Opin Gastroenterol. 2015;31:449–55.
66. Nenci A, Becker C, Wullaert A, et al. Epithelial NEMO links innate immunity to chronic intestinal inflammation. Nature. 2007;446:557–61.
67. Pasparakis M. Regulation of tissue homeostasis by NF-[kappa]B signalling: implications for inflammatory diseases. Nat Rev Immunol. 2009;9:778–88.
68. Greten FR, Eckmann L, Greten TF, et al. IKKbeta links inflammation and tumorigenesis in a mouse model of colitis-associated cancer. Cell. 2004;118:285–96.
69. Chen THP, Swarnkar G, Mbalaviele G, Abu-Amer Y. Myeloid lineage skewing due to exacerbated NF-kappaB signaling facilitates osteopenia in Scurfy mice. Cell Death Dis. 2015;6:e1723.
70. Luckheeram RV, Zhou R, Verma AD, Xia B. CD4(+) T cells: differentiation and functions. Clin Dev Immunol. 2012;2012:925135.
71. Yamamoto-Furusho J. Inflammatory bowel disease therapy: blockade of cytokines and cytokine signaling pathways. Curr Opin Gastroenterol. 2018;34:187.
72. Buonocore S, Ahern PP, Uhlig HH, et al. Innate lymphoid cells drive interleukin-23-dependent innate intestinal pathology. Nature. 2010;464:1371–5.
73. Ibanez L, Rouleau M, Wakkach A, Blin-Wakkach C. Gut microbiome and bone. Joint Bone Spine. 2019;86:43–7.
74. Li J, Sarosi I, Cattley RC, et al. Dkk1-mediated inhibition of Wnt signaling in bone results in osteopenia. Bone. 2006;39:754–66.
75. Qiang YW, Barlogie B, Rudikoff S, Shaughnessy JD, Jr. Dkk1-induced inhibition of Wnt signaling in osteoblast differentiation is an underlying mechanism of bone loss in multiple myeloma. Bone. 2008;42:669–80.
76. Semerad CL, Christopher MJ, Liu F, et al. G-CSF potently inhibits osteoblast activity and CXCL12 mRNA expression in the bone marrow. Blood. 2005;106:3020–7.